analytical chemistry

LETTER

pubs.acs.org/ac

Size Exclusion Chromatography for Semipreparative Scale Separation of $Au_{38}(SR)_{24}$ and $Au_{40}(SR)_{24}$ and Larger Clusters

Stefan Knoppe,[†] Julien Boudon,[‡] Igor Dolamic,[†] Amala Dass,[*,§] and Thomas Bürgi[*,†]

[†]Département de Chimie Physique, Faculté des Sciences, University of Geneva, Quai Ernest-Ansermet 30, 1211 Genève 4, Switzerland

[‡]Laboratoire Interdisciplinaire Carnot de Bourgogne, UMR 5209 CNRS/Université de Bourgogne, 9 av. A. Savary, 21078 Dijon Cedex, France

[§]Department of Chemistry and Biochemistry, University of Mississippi, 352 Coulter Hall, University, Mississippi, 38677, United States

Supporting Information

ABSTRACT: Size exclusion chromatography (SEC) on a semipreparative scale (10 mg and more) was used to size-select ultrasmall gold nanoclusters (<2 nm) from polydisperse mixtures. In particular, the ubiquitous byproducts of the etching process toward $Au_{38}(SR)_{24}$ (SR, thiolate) clusters were separated and gained in high monodispersity (based on mass spectrometry). The isolated fractions were characterized by UV−vis spectroscopy, MALDI mass spectrometry, HPLC, and electron microscopy. Most notably, the separation of $Au_{38}(SR)_{24}$ and $Au_{40}(SR)_{24}$ clusters is demonstrated.

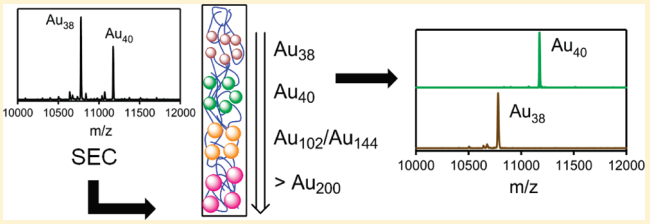

Thiolate-protected gold nanoclusters are an intensively studied field in both nanochemistry and materials sciences. Clusters in a size-regime up to ∼200 atoms show distinct, molecular features, in contrast to their bigger counterparts (>2 nm), which show localized surface plasmon resonances.[1] Synthesis of clusters of defined sizes is challenging and, despite that there has been remarkable progress, often leads to polydisperse product mixtures. Size-focusing has been shown to lead to clusters of high monodispersity.[2,3] Applications of gold nanoclusters lie in fields such as catalysis, sensoring, and drug delivery.[4]

Despite the direct synthesis of polydisperse thiolate-protected gold nanoclusters ($Au_n(SR)_m$; SR: thiolate) in the two-phase Brust−Schiffrin approach,[5,6] a new strategy, size-focusing, has been employed to gain highly monodisperse clusters.[2,3] This involves initial synthesis of clusters, usually polydisperse, followed by etching of the clusters in excess thiols. In the case of $Au_{25}(SR)_{18}$ clusters, it is performed in one step,[7,8] in the case of $Au_{38}(SR)_{24}$[9,10] and $Au_{144}(SR)_{60}$,[11] a two-step procedure is required. Size-focusing often involves heating of the reaction mixtures.

Size-focusing often leads to monodisperse clusters, but the distribution of product clusters strongly depends on several factors: (I) size-distribution of the starting material; (II) reaction time and conditions (temperature); (III) thiol/Au ratio; and (IV) solvent system. Therefore, success of the size-focusing step is not guaranteed and yields may vary. In the worst case, amorphous gold is produced, especially in thermal etching procedures. Repeated attempts may be necessary to gain the desired cluster in required yields and purity.

It was shown that monodisperse clusters can be obtained by separation processes, such as fractionated precipitation,[6,12] size exclusion column chromatography (SEC),[13−15] HPLC,[16] and gel electrophoresis.[17,18] These approaches might help to isolate the desired products from size-focusing attempts that did not work as well as expected but delivered a high proportion of the product. Though fractionated precipitation works on a preparative scale, it yields only rough fractions. Gel electrophoresis has been applied for isolation of monodisperse clusters, but it is restricted to water-soluble specimens. In contrast, HPLC is restricted to analytical quantities. The possibility to use SEC for size-separation was shown, even on a large scale. However, the products were not analyzed by mass spectrometry to confirm monodispersity,[13,15] or SEC was only performed on the analytical scale.[14]

In this report, we present an efficient approach toward size separation of etching products. We chose the thermal etching process toward $Au_{38}(SR)_{24}$ clusters (SR: 2-phenylethanethiolate). It is known that Au_{38} clusters are often accompanied by $Au_{40}(SR)_{24}$ clusters as well as heavier species.[19,20] We demonstrate the separation abilities of charge-neutral styrene divinylbenzene beads at low cross-linkage (1%) on a semipreparative scale.[21] These gels can be operated with common organic solvents (e.g., tetrahydrofuran, toluene) and are specified to have exclusion limits from 600−14 000 Da (note that these values are given for globular proteins in benzene-swollen beads). Since in SEC the hydrodynamic volume of the analyte is a determining factor, it is

Received: March 29, 2011
Accepted: May 24, 2011
Published: May 24, 2011

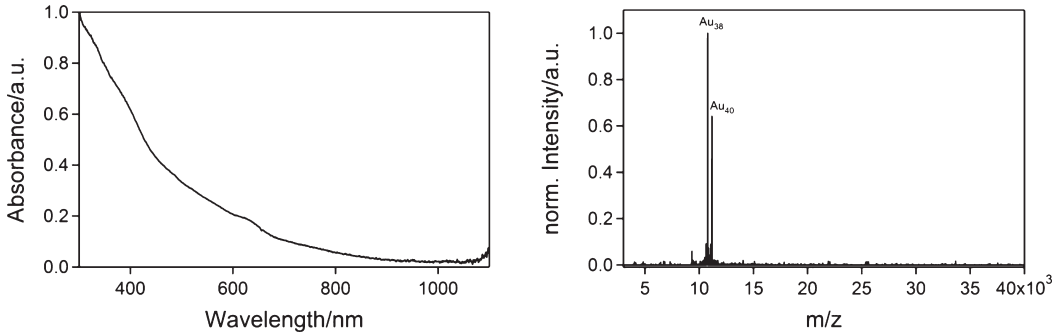

Figure 1. (left) UV−vis spectrum of the crude cluster mixture after thermal etching containing $Au_{38}(CH_2CH_2Ph)_{24}$ clusters prior to size separation. Only some characteristic shoulders indicate the presence of Au_{38} in the sample, most notably at 625 nm. (right) MALDI-MS spectrum of the crude cluster mixture after thermal etching containing $Au_{38}(CH_2CH_2Ph)_{24}$ clusters prior to size separation. Spectra were gained using a DCTB matrix at the laser threshold.

expected that clusters of higher mass than the specified exclusion limit can be separated. The eluted clusters are characterized with MALDI mass spectrometry, UV−vis spectroscopy, and transmission electron microscopy (TEM).

EXPERIMENTAL SECTION

General Remarks. The origin of the materials used and the synthesis of glutathionate-protected clusters and core etching toward $Au_{38}(SR)_{24}$ are described in the Supporting Information.

Size Exclusion Chromatography. A total of 45 g of BioRad BioBeads S-X1 were suspended in 400 mL of tetrahydrofuran and allowed to swell overnight. The swollen beads were put into a column (2 cm in diameter) equipped with a glass frit (G4), allowed to settle under a gentle stream of N_2, and washed with several bed volumes of THF until a constant height (90 cm) was reached. The polydisperse clusters (40 mg in a minimum amount of solvent) were eluted at 0.5−1 mL/min and collected in gross fractions (**1**, **2**, **3**, and **4**; according to decreasing elution times or increasing particle size; see below). These fractions were further purified in individual runs. After elution, the solvent was evaporated in vacuo, and the product was washed with methanol, redissolved in methylene chloride, and filtered over a PTFE syringe filter (0.2 μm). For all separations, the same column was used and washed with several bed volumes of THF prior to reuse to wash out impurities. The column was stored under inert gas; this prevents decomposition of the stationary phase (bleeding) and enhances the lifetime of the column. Retention factors $k(\mathbf{n})$ (**n**, fraction **1**, **2**, **3**, **4**) were determined as follows: a pure sample of the individual fractions **1**−**3** was mixed with some fraction **4** (which is assumed to travel at the speed of the solvent) as an internal reference, and the retention times $t_R(\mathbf{n})$ were measured. The reduced retention times $t_R'(\mathbf{n}) = t_R(\mathbf{n}) - t_R(\mathbf{4})$ were calculated to give the retention factors $k(\mathbf{n}) = t_R'(\mathbf{n})/t_R(\mathbf{4}) = t_R'(\mathbf{n})/t_R(\mathbf{solvent})$.

UV−Visible Spectroscopy. UV−vis spectra were recorded on an Avantes AvaSpec-2048 and a Varian Cary 50 UV−vis spectrophotometer. All spectra were either recorded in methylene chloride or tetrahydrofuran, and a quartz cell of 1 cm path length was used. For comparison, all spectra were normalized at 300 nm, if not mentioned otherwise.

MALDI Analysis. Mass spectra were obtained using a Bruker Autoflex mass spectrometer equipped with a nitrogen laser at near threshold laser fluence in positive linear mode. 3-(4-*tert*-Butylphenyl)-2-methyl-2-propenylidene]malononitrile (DCTB) was used as the matrix with a 1:1000 analyte−matrix ratio. A volume of 2 μL of the analyte−matrix mixture was applied to the target and air-dried.

Transmission Electron Microscopy. For preparation of the samples, a diluted solution of particles in methylene chloride was dropcast on a carbon coated TEM grid (Cu, 300 mesh, Electron Microscopy Sciences, Hatfield, PA) and allowed to dry in air. TEM observations were performed on a JEOL JEM-2100 LaB6 microscope operating at 200 kV.

HPLC. High-performance liquid chromatography was performed on a JASCO 20XX plus series system. A Phenomenex Luna 5 μ PFP(2) (PFP, pentafluorophenyl) 100 Å column (250 mm × 4.60 mm) was used, and the eluting analytes were detected with a JASCO UV-2070 plus UV−visible detector at 400 nm. The samples were dissolved in toluene, and the best results were gained using pure toluene as the eluent at a flow rate of 0.5 mL/min. We also tried mixtures of acetone and toluene at different ratios and flow rates as well as gradient elution. All these variations had no significant influence on the separation. All chromatograms were measured at room temperature.

RESULTS AND DISCUSSION

Synthesis of the Crude Clusters. Glutathionate-protected clusters and the subsequent etching step toward crude $Au_{38}(CH_2CH_2Ph)_{24}$ were performed according to the literature.[20] As it is an intrinsic property of core etching in excess thiol, the initial clusters have to be considerably bigger than the desired product. Success of the etching step strongly depends on the size-distribution of the starting material, thiol/Au ratio, temperature, and time.[2] Since the control of size distribution in the starting material is hard to achieve (and therefore each reaction batch leads to different size distributions), the product distribution after etching varies. In the following, we demonstrate the power of size exclusion chromatography toward highly monodisperse clusters in semipreparative yields.

The glutathionate-protected clusters were dissolved in water and mixed with a huge excess of 2-phenylethanethiol and acetone, which acts as a phase transfer agent. The reaction mixture was heated to 80 °C for 3 h and the clusters were transferred to the organic phase. During the thermal etching, a white, insoluble material formed, presumably Au-thiolate polymers. The clusters were extracted with methylene chloride, concentrated, and precipitated from methanol. Several washing and filtration cycles were applied to remove free thiols and other

dx.doi.org/10.1021/ac200789v |*Anal. Chem.* 2011, 83, 5056–5061

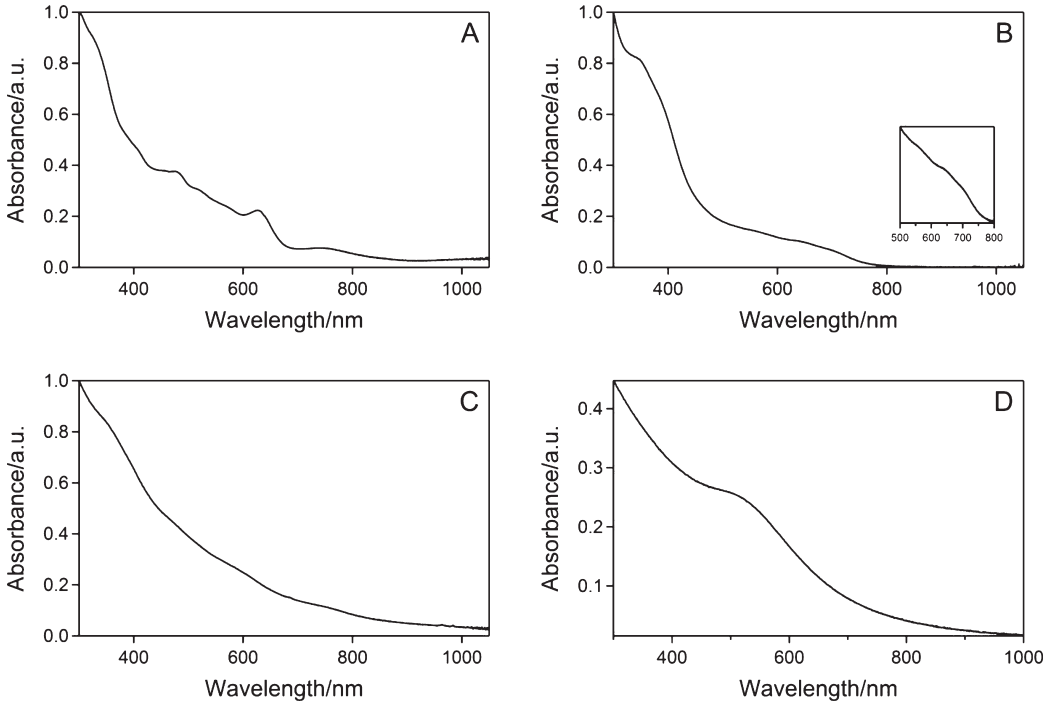

Figure 2. (A) UV−vis spectrum of isolated $Au_n(SCH_2CH_2Ph)_m$(**1**) gained from thermal etching after SEC. The shape of the spectrum indicates presence of highly monodisperse $Au_{38}(SCH_2CH_2Ph)_{24}$ clusters; (B) UV−vis spectrum of isolated $Au_n(SCH_2CH_2Ph)_m$(**2**) gained from thermal etching after SEC. The shape of the spectrum is reminiscent of monodisperse $Au_{40}(SCH_2CH_2Ph)_{24}$ clusters, which is confirmed by MALDI mass spectrometry, see below; (C) fraction **3**, reminiscent of $Au_{144}(SR)_{60}$; (D) fraction **4** shows a localized surface plasmon resonance, indicating bigger particles. This spectrum was not normalized.

byproducts. A UV−vis spectrum of the purified crude clusters is shown in Figure 1. During the methanol washing procedures, we noticed that a fraction of clusters does not immediately precipitate and is washed away during the filtration process. Judging from its UV−vis spectrum, the filtrate consists of $Au_{25}(SR)_{18}$ clusters (spectrum not shown here). This fraction is not further considered in the following. However, quick washing with methanol enables effective separation of Au_{25} clusters from bigger species. Formation of Au_{25} might be due to very small glutathionate-protected clusters of sizes below the threshold limit of ∼40 Au atoms.

Size Exclusion Chromatography. The crude cluster mixture (∼40 mg) was size-separated on a size exclusion column using BioRad BioBeads S-X1 as the stationary phase. According to the supplier of the beads, particle sizes are 40−80 μm. Tetrahydrofuran was used as the eluent. The clusters were first collected into four rough fractions which are assigned according to increasing masses (decreasing elution times) as **1**, **2**, **3**, and **4**, respectively. Each of these fractions was then further purified by repeated SEC cycles until no further separation was observable (constant UV−vis spectra). As in all chromatographic processes, the analyte should be dissolved in a minimum amount of solvent in order to keep the injected trace as defined as possible. The individual fractions were characterized by UV−vis spectroscopy and MALDI mass spectrometry. The same column was used for all separation cycles. The packed column was stored under inert gas and an excess of solvent. We noticed that protection from light is not needed, and the column still separates clusters even weeks after packing. More than 20 SEC runs can be performed on one column without loss of separation power.

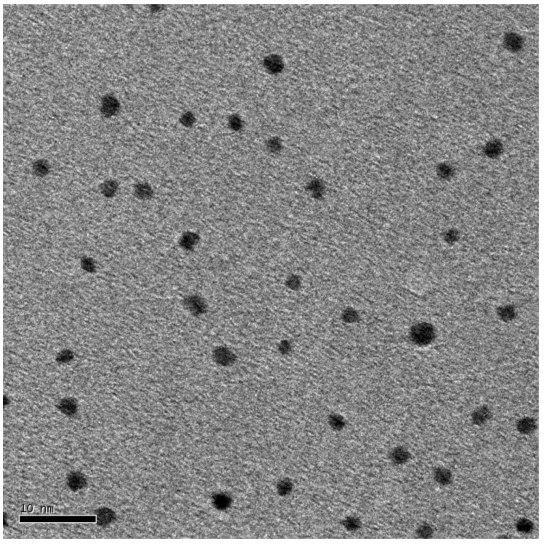

Figure 3. Transmission electron micrograph of particles isolated as fraction **4**. The particles have sizes of ∼2.5 ± 0.1 nm. The scale bar is 10 nm (for details of particle size determination, see the Supporting Information).

Fraction **4** elutes first, and the band is clearly separated from others, as these overlap. Fraction **1**, eluting last, is easily purified by collecting the very last part of the band and repeating this procedure. Similarly, fraction **3** is isolated by collecting the first part of the band. Fraction **2** is most complicated to purify, since it overlaps with both **1** and **3**; in this case, one has to be quite strict

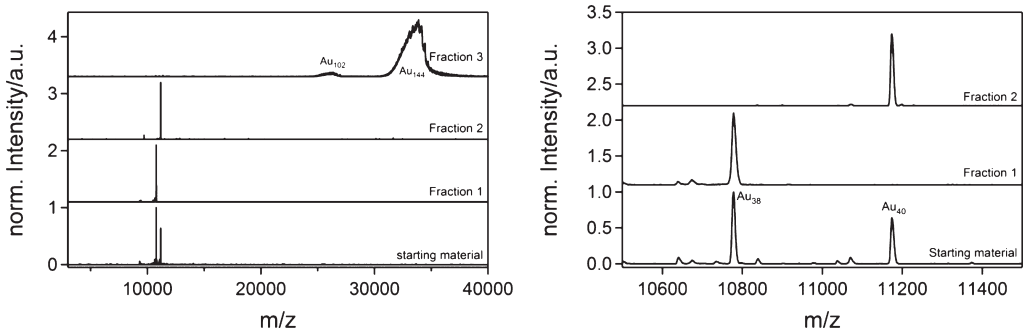

Figure 4. (left) MALDI mass spectra of the crude clusters, fractions **1**, **2**, and **3**; (right) zoom into the Au_{38}/Au_{40} region (10 kDa) of the starting material and fractions **1** and **2**. The absence of clusters of higher mass than Au_{40} in the starting material is due to ionization effects. Monodispersity after SEC separation is indicated by the absence of other signals except from Au_{38} (**1**) and Au_{40} (**2**), respectively.

with the cutoff. Exemplary photographs are shown in the Supporting Information (Figure S-1). The described procedure is repeated for the individual fractions, which leads to gradual narrowing of dispersity. Typically, 5−6 cycles were applied per fraction (except for fraction **4**, which is regarded as "pure" after the first run). In the case of **4**, we assume that the particles have sizes above the exclusion limit and cannot be purified by further chromatography (Note that this does not mean monodispersity in this case!). This explains the clearly visible gap between **4** and **3**, as the latter is assumed to be within the exclusion limits. With dependence on the compound, a SEC run needs 2.5 (fraction **4**) to 4 h (fraction **1**). For fraction **1**, ∼12 mg were yielded, for fraction **2** ∼8 mg; the yields for the other fractions were not determined. Note that the isolated yields and the number of chromatography runs may vary as they depend on the size-distribution of the crude material. We determined retention factors $k(\mathbf{n})$ for each fraction, using fraction **4** as the internal standard, since we assume that **4** passes the column at the speed of the solvent. For this, a pure sample of the individual fractions **1**−**3** were mixed with fraction **4** and separated. The elution times $t_R(\mathbf{n})$ were noted and $k(\mathbf{n}) = (t_R(\mathbf{n}) - t_R(\mathbf{4}))/t_R(\mathbf{4})$ was calculated. Per definition, $k(\mathbf{4})$ is 0; $k(\mathbf{3})$ was determined to be 0.2−0.35; $k(\mathbf{2})$ = 0.35−0.45, and $k(\mathbf{1})$ = 0.4−0.6 (these values cover the whole bands). Since the values are close, it becomes obvious that several chromatographic cycles have to be applied to yield pure fractions.

UV−Visible Spectroscopy and TEM. UV−vis spectra of fractions **1**, **2**, **3**, and **4** are shown in Figure 2 (photographs are shown in Figure S-2 in the Supporting Information). Fraction **1** shows distinct signals (485, 625, and 755 nm), which are clearly assignable to the well-known spectrum of Au_{38} clusters. Fraction **2** gives an olive-green solution in both THF and methylene chloride. The absorption onset lies at ∼800−850 nm and several (weak) shoulders (340, 550, 635, and 685 nm) can be identified, suggesting monodispersity. The UV−vis spectrum of fraction **3** has an onset >1000 nm. The spectrum shows several shoulders, and the spectrum is reminiscent of that of $Au_{144}(SR)_{60}$ clusters.[11] A broad absorbance can be observed in the UV−vis spectrum of fraction **4**, at a maximum of ∼500 nm. The particles dissolve as a gray-red solution and we therefore conclude that this fraction mainly consists of small plasmonic particles. TEM images were recorded for fraction **4** (Figure 3). The particles are small in diameter (∼2.5 ± 0.1 nm) and a narrow size-distribution is found (Figure S-3 in the Supporting Information), though the particles are not perfectly monodisperse. Sizes of 2 nm are widely regarded as being a threshold to exhibit a localized surface plasmon resonance.

Mass Spectrometry. MALDI mass spectra of the crude sample as well as of **1**, **2**, and **3** were recorded using a DCTB matrix, which produces signals of unfragmented clusters.[22,23] The crude product shows signals for $Au_{38}(SCH_2CH_2Ph)_{24}$ (m/z = 10 778, calcd 10 778, used as an internal reference) and $Au_{40}(SCH_2CH_2Ph)_{24}$ (m/z = 11 174, calcd 11 172) (Figure 1) at a ratio of ∼3:2. The Au_{40} cluster is a common byproduct of the etching process toward Au_{38}.[19,20] Signals of higher mass only occur in traces as well as Au_{25} clusters at m/z = 7391. The mass spectra of the isolated fractions **1** and **2** show only one signal each, at m/z = 10 778 and 11 174, respectively (Figure 4). The MALDI mass spectrum indicates that fraction **3** consists of $Au_{102}(SR)_{44}$ and $Au_{144}(SR)_{60}$ (calcd, 26 128 and 36 597, respectively; found, ∼26 000 and 30 000−35 000).[12] It was suggested that the signals are broadened due to ionization problems.[22] With increasing core size, gold nanoclusters tend to show broadening in the MALDI signals, which is ascribed to less efficient charge transfer from the matrix to the analyte and less sensitive detectors at higher masses. Fraction **4** was not analyzed, since the plasmonic particles are too heavy for MALDI analysis.

HPLC. Fractions **1** and **2** were further analyzed by HPLC measurements (both pure and purposely mixed).[16] Following the method of Jimenez et al, we examined toluene and acetone at different ratios and flow rates.[16a] Gradient elution (100−0% toluene) was tried as well. Among the tested conditions, best results were gained using pure toluene as the eluent at a flow rate of 0.5 mL/min. As shown in Figure 5, pure Au_{38} and Au_{40} clusters (pure in this context based on MALDI spectra) show slightly different retention times at the peak maxima (5.21 and 5.25 min for Au_{38} and Au_{40}, respectively); when purposely mixed, the retention time decreases slightly (5.15 min). Apart from the peak stemming from the clusters, no significant signal was observed (detection at 400 nm). UV−vis spectra were measured at the peak maxima of the pure samples. For pure Au_{38} and Au_{40}, the spectra have shapes as expected (Figure 6). In the mixture, we measured spectra at the beginning and the end of the peak, in order to see whether the spectrum of the peak changes with retention time and the peak consists more of an overlap between two individual peaks than eluting as a fully nonseparated mixture. The UV−vis spectra were measured at 5.02 and 5.32 min, expecting to see more Au_{38} in the first and more Au_{40} character in the latter one. Interestingly, the characteristics of the spectra are reversed, in a mixture, Au_{40} seems to elute at lower retention times than Au_{38}. Under the applied conditions, affinity chromatography cannot separate Au_{38} and Au_{40} and act as a test for true monodispersity. This is in agreement with the literature,[16b]

dx.doi.org/10.1021/ac200789v |*Anal. Chem.* 2011, 83, 5056–5061

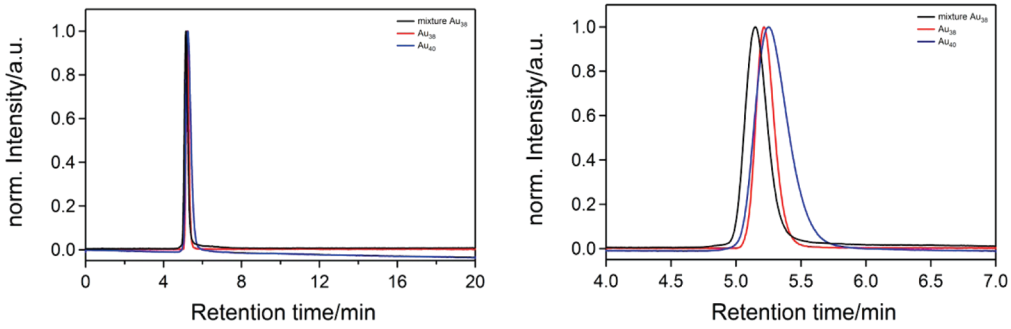

Figure 5. (left) HPLC chromatogram (toluene, 0.5 mL/min, 25 °C) of fractions 1 (red), 2 (blue), and a mixture of these (black). (Right) zoom into the peak region. The mixture between Au_{38} and Au_{40} shows a slightly shorter retention time than the individual clusters, which themselves differ only slightly.

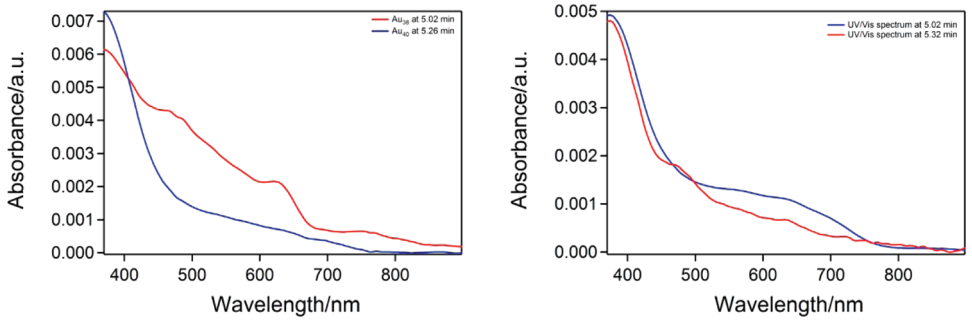

Figure 6. (left) UV−vis spectra of fractions 1 (red) and 2 (blue) at peak maxima during HPLC; (right) UV−vis spectra of purposely mixed fractions 1 and 2 after 5.02 (blue) and 5.32 min (red; spectra not normalized). The two spectra clearly show characteristics of Au_{40} and Au_{38}, respectively. Note, that the retention times in the mixture seem to be reversed when compared to the pure samples.

where a broad peak is found in chromatograms and the corresponding UV−vis spectrum resembles more of impure Au_{38} than of truly monodisperse clusters (see ref 16b; Figures 1 and 3, peak 5). Future work might lead to optimization of conditions that can discriminate between Au_{38} and Au_{40}.

The MALDI signals found for fractions **1** and **2** are unambiguously assignable to Au_{38} and Au_{40} clusters, respectively. This is in agreement with UV−vis data. No impurities are identified in the MALDI mass spectra; no byproducts are found in HPLC, though HPLC cannot fully discriminate between Au_{38} and Au_{40}. We therefore deem that size exclusion chromatography can be used as an effective method for the separation of clusters differing only in two gold atoms (at least at MALDI sensitivity). The technique yields monodisperse clusters on a 10 mg scale. Note that only repeated runs on the SEC lead to monodisperse samples. Since size exclusion chromatography is based rather on the hydrodynamic volume of the sample than on its mass (that is usually given as an estimated cutoff to characterize a gel), we anticipate that the difference of two gold atoms in the cluster cores of Au_{38} and Au_{40} leads to considerably different structures.

Products of thermal etching processes have been described as a result of a "survival of the robustest" principle.[2] Comparing the relative intensities of Au_{38} and Au_{40} signals in the original sample (~3:2, the ratio may vary depending on the conditions of the etching process), we also propose that Au_{40} is not just a byproduct of thermal etching but should rather be treated as a cluster of a stability similar to that of Au_{38}. Little is known about this cluster. With the application of the concept of bridged binding between gold and thiolate ligands in long and short staples,[24] it was proposed that the $Au_{40}(SR)_{24}$ cluster possesses a Au_{26} core and is ligated by six $Au(SR)_2$ and four $Au_2(SR)_3$ staples.[20] It appears to be charge neutral, and it is a $16e^-$ cluster in terms of the magic number concept. Since 16 is not a magic number itself, its core structure should not be spherical.[25]

CONCLUSIONS

We demonstrated the separation of thiolate-protected gold nanoclusters using size exclusion chromatography on a semipreparative scale. Repeated runs allow isolation of fractions up to ~Au_{144} in high monodispersity for Au_{38} and Au_{40} and gives mixtures of clusters of higher mass. Most notably, the separation of clusters of relatively low mass difference (Au_{38}/Au_{40}) is possible (on MALDI sensitivity), allowing access to greater amounts (10 mg and more) of highly pure clusters for further studies.

The column, once packed, can be reused more than 20 times without significant loss of separation power. This makes the method advantageous under both economical and ecological aspects. Access to different cluster sizes from one reaction batch also minimizes the risks of size-focusing that is often accompanied by trial-and-error, since the product distribution depends on the size distribution of the starting material.

ASSOCIATED CONTENT

Supporting Information. Synthesis of the starting material, photographs of the isolated fractions, and further information on electron microscopy. This material is available free of charge via the Internet at http://pubs.acs.org.

AUTHOR INFORMATION

Corresponding Author

*E-mail: Amal@olemiss.edu (A.D.); Thomas.Buergi@unige.ch (T.B.).

ACKNOWLEDGMENT

We gratefully acknowledge financial support from the University of Geneva (S.K., T.B.) and from NSF Grant 0903787 and University of Mississippi Startup Fund (A.D.). We thank Charles Hussey, College of Liberal Arts, for the Bruker Autoflex MALDI TOF instrumentation support and P. Nimmala for preliminary experiments.

REFERENCES

(1) Jin, R. *Nanoscale* **2010**, *2*, 343–362.
(2) Jin, R.; Qian, H.; Wu, Z.; Zhu, Y.; Zhu, M.; Mohanty, A.; Garg, N. *J. Phys. Chem. Lett.* **2010**, *1*, 2903–2910.
(3) Schaaff, T. G.; Whetten, R. L. *J. Phys. Chem. B* **1999**, *101*, 9394–9396.
(4) Zhu, Y.; Qian, H.; Drake, B. A.; Jin, R. *Angew. Chem., Int. Ed.* **2010**, *49*, 1295–1298.
(5) Brust, M.; Walker, M.; Bethell, D.; Schiffrin, D. J.; Whyman, R. *J. Chem. Soc., Chem. Commun.* **1994**, 801–802.
(6) Price, R. C.; Whetten, R. L. *J. Am. Chem. Soc.* **2005**, *127*, 13750–13751.
(7) Wu, Z.; Suhan, J.; Jin, R. *J. Mater. Chem.* **2009**, *19*, 622–626.
(8) Dharmaratne, A. C.; Krick, T.; Dass, A. *J. Am. Chem. Soc.* **2009**, *131*, 13604–13605.
(9) Tokkainen, O.; Ruiz, V.; Rönnholm, G.; Kalkinnen, N.; Liljeroth, P.; Quinn, B. M. *J. Am. Chem. Soc.* **2008**, *130*, 11049–11055.
(10) Qian, H.; Zhu, Y.; Jin, R. *ACS Nano* **2009**, *3*, 3795–3803.
(11) Qian, H.; Jin, R. *Nano Lett.* **2009**, *9*, 4083–4087.
(12) Whetten, R. L.; Khoury, J. T.; Alvarez, M. M.; Murthy, S.; Vezmar, I.; Wang, Z. L.; Stephens, P. W.; Cleveland, C. L.; Luedtke, W. D.; Landmann, U. *Adv. Mater.* **1996**, *8*, 428–433.
(13) (a) Siebrands, T.; Giersig, M.; Mulvaney, P.; Fischer, C.-H. *Langmuir* **1993**, *9*, 2297–2300. (b) Wilcoxon, J. P.; Martin, J. E.; Provencio, P. *Langmuir* **2000**, *16*, 9912–9920.
(14) Tsunoyama, H.; Negishi, Y.; Tsukuda, T. *J. Am. Chem. Soc.* **2006**, *128*, 6036–6037.
(15) (a) Gautier, C.; Taras, R.; Gladiali, S.; Bürgi, T. *Chirality* **2008**, *20*, 483–493. (b) Frein, S.; Boudon, J.; Vonlanthen, M.; Scharf, T.; Barberá, J.; Süss-Fink, G.; Bürgi, T.; Dechenaux, R. *Helv. Chim. Acta* **2008**, *91*, 2321–2337.
(16) (a) Jimenez, V. L.; Leopold, M. C.; Mazzitelli, C.; Jorgenson, J. W.; Murray, R. W. *Anal. Chem.* **2003**, *75*, 199–206. (b) Song, Y.; Jimenez, V.; McKinney, C.; Donckers, R.; Murray, R. W. *Anal. Chem.* **2003**, *75*, 5088–5096. (c) Choi, M. M. F.; Douglas, A. D.; Murray, R. W. *Anal. Chem.* **2006**, *78*, 2779–2785. (d) Zhang, Y.; Shuang, S.; Dong, C.; Lo, C. K.; Paau, M. C.; Choi, M. M. F. *Anal. Chem.* **2009**, *81*, 1676–1685.
(17) Schaaff, T. G.; Knight, G.; Shafigullin, M. N.; Borkman, R. F.; Whetten, R. L. *J. Phys. Chem. B* **1998**, *102*, 10643–10646.
(18) Gautier, C.; Bürgi, T. *J. Am. Chem. Soc.* **2006**, *133*, 11079–11087.
(19) Qian, H.; Zhu, Y.; Jin, R. *J. Am. Chem. Soc.* **2010**, *132*, 4583–4585.
(20) Knoppe, S.; Dharmaratne, A. C.; Schreiner, E.; Dass, A.; Bürgi, T. *J. Am. Chem. Soc.* **2010**, *132*, 16783–16789.
(21) Bio-Rad Laboratories. Bio Beads S-X Beads Gel Permeation Chromatography Instruction Manual, Rev C.
(22) Harkness, K. M.; Cliffel, D. E.; McLean, J. A. *Analyst* **2010**, *135*, 868–874.
(23) Dass, A.; Stevenson, G. R.; Tracy, J. B.; Murray, R. W. *J. Am. Chem. Soc.* **2008**, *130*, 5940–5946.
(24) Häkkinen, H.; Walter, M.; Grönbeck, H. *J. Phys. Chem. B* **2006**, *110*, 9927–9931.
(25) Walter, M.; Akoola, J.; Lopez-Acevedo, O.; Jadzinsky, P. D.; Calero, G.; Ackerson, C. J.; Whetten, R. L.; Grönbeck, H.; Häkkinen, H. *Proc. Natl. Acad. Sci. U.S.A.* **2008**, *105*, 9157–9162.